

Fixed-delay Interferometry for Doppler Extra-solar Planet Detection

Jian Ge

Department of Astronomy and Astrophysics, Penn State University, University Park, PA 16802; Email: jian@astro.psu.edu

ABSTRACT

We present a new technique based on fixed-delay interferometry for high throughput, high precision and multi-object Doppler radial velocity (RV) surveys for extra-solar planets. The Doppler measurements are conducted through monitoring the stellar fringe phase shifts of the interferometer instead of absorption line centroid shifts as in state-of-the-art echelle spectroscopy. High Doppler sensitivity is achieved through optimizing the optical delay in the interferometer and reducing photon noise by measuring multiple fringes over a broadband. This broadband operation is performed through coupling the interferometer with a low to medium resolution post-disperser. The resulting fringing spectra over the band pass are recorded on a 2-D detector, with fringes sampled in the slit spatial direction and the spectrum sampled in the dispersion direction. The resulting total Doppler sensitivity is, in theory, independent of dispersing power of the post-disperser, which allows development of new generation RV machines with much reduced size, high stability and low cost compared to echelles. This technique has the potential to improve RV survey efficiency by 2-3 orders of magnitude over cross-dispersed echelle spectroscopy approach to allow a full sky RV survey of hundreds of thousands of stars for planets, brown dwarfs, and stellar companions once the instrument is operated as a multi-object instrument and optimized for high throughput. The simple interferometer response potentially allows this technique to be operated at other wavelengths independent of popular iodine reference sources, being actively used in most of the current echelles for Doppler planet searches, to search for planets around early type stars, white dwarfs, and M, L and T dwarfs for the first time. The high throughput of this instrument could also allow investigation of extra-galactic objects for RV variations at high precision.

Subject headings: instrumentation: interferometers – planetary systems – techniques: radial velocities

1. Introduction

Interferometer techniques based on variable optical delays have already been proposed for high precision RV measurements (Connes 1985; Fradsen et al. 1993; Douglas 1997), the most recent of which is Holographic Heterodyning Spectroscopy (HHS). To our knowledge, none of these techniques has yet achieved RV precision on a par with cross-dispersed echelle spectroscopy (~ 3 m/s) (Butler et al. 1996). The fundamental limitation of interferometric techniques is the narrow band pass (e.g. ~ 30 Å) compared to the broadband operation of the echelle (~ 1000 Å), which provides ~ 6 times higher Doppler error than the echelles at the same spectral resolution.

The narrow band limitation can be overcome by a new kind of interferometer approach based on a fixed optical delay and a post-disperser. Fixed-delay interferometers with narrow band passes have been used in high precision RV measurements in solar astrophysics since 1980's (Title & Ramsey 1980; Harvey et al. 1995; Kozhevnikov et al. 1995; 1996). The best RV precision of ~ 3 m/s has been reported with solar observations (Kozhevnikov et al. 1995; 1996). Recent laboratory work with a wide angle Michelson interferometer with a fixed delay and a medium resolution grating post-disperser appears to offer ~ 1 m/s RV precision, similar to the echelle spectroscopy (Erskine & Ge 2000). The first light of a prototype instrument based on this concept at the Hobby-Eberly 9 m and Palomar 5 m telescopes in 2001 demonstrates that ~ 8 m/s RV precision has been achieved with stellar observations (Ge et al. 2001; van Eyken et al. 2001; Ge et al. 2002). Here we present the theoretical principle behind this new RV technique, its performance comparison with the cross-dispersed echelle technique and its new capability for all sky RV surveys for extra-solar planets.

2. Principle of Fixed-delay Interferometry

This new approach is illustrated in Figure 1. The circular incoming beam from a telescope is converted to a rectangular one by cylindrical optics, split into two beams with equal amplitude and fed to an interferometer with a fixed optical delay in one of the arms to form fringes in stellar absorption lines. The uncorrelated fringes over a broadband (white fringes) are separated by a post-disperser and recorded on a 2-D detector array with fringes sampled on the slit spatial direction and the spectrum sampled in the dispersion direction. This post-disperser can be any dispersing device (e.g. grating, prism, grism, Fabry-Perot interferometer). The fringe period in the slit spatial direction is proportional to wavelength. Therefore, fringes over a bandwidth similar to, or larger than, that of the echelles can be properly sampled and measured on a suitable detector array (e.g. CCD), which can help reduce RV measurement noise due to photon statistics.

In this interferometer, high contrast interference fringes are formed when the optical path difference is within the coherence length (Goodman 1984). Parallel fringes are created when the faces of the two interferometer mirrors are slightly tilted with respect to each other. The interference order, m , is determined by

$$m\lambda = d, \quad (1)$$

where d is the total optical delay, and λ is the operating wavelength. Once the delay is fixed, Doppler RV motion will shift the fringes to different orders. The corresponding Doppler velocity shift, Δv , is

$$\Delta v = \frac{c\lambda}{d} \Delta m. \quad (2)$$

The Doppler analysis is performed on the “normalized” fringe (i.e., divided by the continuum), which can be represented as a function of velocity

$$I = 1 + \gamma_i \sin\left(2\pi \frac{v}{c\lambda/d} + \phi_0\right), \quad (3)$$

where γ_i is the fringe visibility, and ϕ_0 is the phase value for the first pixel of the fringe. Along the fringe, the average uncertainty in the velocity from one pixel is

$$\sigma_p = \left\langle \frac{\epsilon_I}{dI/dv} \right\rangle \approx \frac{c\lambda}{4d\gamma_i(S/N)}, \quad (4)$$

where ϵ_I is the uncertainty in the residual intensity at the pixel, for a normalized spectrum, $\epsilon_I = 1/(S/N)$, where (S/N) is the signal-to-noise ratio at the pixel, and the average slope over one side of the fringe (half period) of the sinusoidal interferometer response

$$\left\langle \frac{dI}{dv} \right\rangle = \frac{4d\gamma_i}{c\lambda} \quad (5)$$

is used. If an interference fringe is sampled by N_{pix} pixels, then the total intrinsic Doppler error under photon noise limits is

$$\sigma_{f,i} \approx \frac{c\lambda}{4d\gamma_i\sqrt{F_i}}, \quad (6)$$

where $(S/N) = \sqrt{N_{ph}}$ is applied, N_{ph} is the number of photons received by each pixel, and $F_i = N_{pix}N_{ph}$ is the total photon number collected by each fringe. It is clear that the Doppler precision in the interferometer approach is determined by delay, visibility, and total photons collected in each fringe. If we simply assume that each stellar intrinsic absorption line is a Gaussian shape with a FWHM of $\Delta\lambda_i$ and a depth of D_i ($0 \leq D_i \leq 1$), then the visibility as a function of optical delay can be derived (Goodman et al. 1984) as

$$\gamma_i = D_i e^{-3.56 \frac{d^2}{l_c^2}}, \quad (7)$$

where $l_c = \lambda^2/\Delta\lambda_i$ is the coherence length of the interferometer beam. A simple derivation shows that $(d\gamma_i)$ reaches a maximum value of $0.23D_i l_c$, when $d = 0.37l_c$ as shown in Figure 2. Therefore, the minimum intrinsic Doppler error per fringe is

$$\sigma_{f,i} \approx \frac{1.1c\lambda}{D_i l_c \sqrt{F_i}}, \quad (8)$$

This formula indicates that the intrinsic Doppler error for each fringe decreases with increasing coherence length of the light, the flux per fringe and also with increasing absorption line depth. If multiple fringes (N_i) over a broadband are used for Doppler RV measurements, then the total Doppler error is

$$\sigma_{f,i,t} \approx \frac{1}{\sqrt{N_i}} \frac{1.1c\lambda}{D_i l_c \sqrt{F_i}}, \quad (9)$$

assuming line depths, widths, and F_i are the same for all fringes. For the multiple fringe measurements, the intrinsic line profiles are convolved with the response of the post-disperser, which affects RV precision. Assuming that the post-disperser response profile is approximately a Gaussian function with a FWHM of $\Delta\lambda_g$, the FWHM of the observed line is $\Delta\lambda_o \approx \Delta\lambda_g$ if $\Delta\lambda_g \gg \Delta\lambda_i$. The observed absorption line depth is

$$D_o \approx \frac{\Delta\lambda_i}{\Delta\lambda_o} D_i. \quad (10)$$

The observed flux within each fringe (or absorption line) is increased to

$$F_o \approx \frac{\Delta\lambda_o}{\Delta\lambda_i} F_i. \quad (11)$$

The total measured Doppler error per fringe becomes

$$\sigma_{f,o} \approx \sqrt{\frac{\Delta\lambda_o}{\Delta\lambda_i}} \sigma_{f,i}. \quad (12)$$

The Doppler sensitivity for each fringe is decreased due to the use of the post-disperser. However, if the detector dimension in the dispersion direction and the sampling of each resolution element are fixed, then the total number of absorption lines covered by the array, N_o , increases to

$$N_o \approx \frac{\Delta\lambda_o}{\Delta\lambda_i} N_i, \quad (13)$$

if the absorption line density is approximately constant over the wavelength coverage. Therefore, the total Doppler error

$$\sigma_{f,o,t} \approx \frac{1}{\sqrt{N_o}} \frac{1.1c\lambda}{D_o l_c \sqrt{F_o}} \approx \sigma_{f,i,t}. \quad (14)$$

is independent of the resolution of the post-disperser, which is significantly different from the echelle approach and offers new possibilities for Doppler planet searches.

In the cross-dispersed echelle spectroscopy, a total measured Doppler error (photon noise error) for a stellar absorption line with an intrinsic FWHM, $\Delta\lambda_i$, and depth, D_i , at a spectral resolution of $\Delta\lambda_o$ is described as

$$\sigma_{e,o} \approx \left(\frac{\Delta\lambda_o}{\Delta\lambda_i}\right)^{3/2} \frac{c\Delta\lambda_i}{D_i\lambda\sqrt{F_i}} = \left(\frac{\Delta\lambda_o}{\Delta\lambda_i}\right)^{3/2} \sigma_{e,i}, \quad (15)$$

where $\Delta\lambda_o = \sqrt{\Delta\lambda_e^2 + \Delta\lambda_i^2}$, $\Delta\lambda_e$ is the FWHM of the echelle response. For a fixed bandwidth of the echelle, e.g., $\sim 1000 \text{ \AA}$ determined by the bandwidth of iodine absorption in the Visible for calibrations (Butler et al. 1996), the total measured echelle error is

$$\sigma_{e,o,t} \approx \left(\frac{\Delta\lambda_o}{\Delta\lambda_i}\right)^{3/2} \sqrt{\frac{N_i}{N_e}} \sigma_{e,i,t} \approx \left(\frac{\Delta\lambda_o}{\Delta\lambda_i}\right)^{3/2} \sqrt{\frac{N_i}{N_e}} \sigma_{f,o,t}, \quad (16)$$

where the total number of stellar lines covered in this band, N_e , is fixed. This indicates that the Doppler error in the echelle approach strongly depends on the echelle resolving power. At typical echelle resolution such as $R \sim 60,000$ (e.g. Suntzeff et al. 1994; Vogt et al. 1994; D’Odorico et al. 2000), the Doppler error is ~ 1.3 times higher than that in the interferometer approach for the same wavelength coverage and photon flux. Therefore, in order to approach the highest possible Doppler precision, approximately the same as that in the interferometer approach, limited only by the stellar intrinsic line profiles, the spectral resolving power must be much higher than the stellar intrinsic line width, i.e. $\Delta\lambda_e \ll \Delta\lambda_i$.

3. Discussions

The independence of Doppler sensitivity with the post-disperser resolving power in the interferometer approach potentially allows about two to three orders of magnitude improvement in RV survey speed for planets over echelle techniques. The use of low resolution but high efficiency post-dispersers can significantly boost the overall detection efficiency and allow single dispersion order operations for potential multiple object observations. The current echelle instruments are limited to a few percent total detection efficiency, or less; this includes telescope transmission, slit loss, spectrograph and detection loss, due to use of very high resolution echelle and complicated camera optics (Vogt et al. 1994; Suntzeff et al. 1996; D’Odorico et al. 2000). An interferometer coupled with a low resolution dispersing instrument potentially offers perhaps $\sim 30\%$ detection efficiency, 5-10 times higher than the echelle, thus allowing to extend RV survey depth to fainter objects with fixed size telescope. This high efficiency can be achieved because both of the interferometer and low resolution

spectrograph can be optimized for high transmission¹. The potential operation of the instrument in a multi-object mode allows simultaneous observations of hundreds of objects in a single exposure with broadband coverage on a large 2-D detector array. Full sky coverage of an RV survey for planets becomes possible with a wide field telescope.

In addition, the simple response function potentially offers lower systematic errors than those echelle approaches. Currently, the systematic errors associated with the echelle instrument response account for about 2 m/s Doppler error largely due to the de-convolution of observed stellar spectra to create star templates (Butler et al. 1996; Valenti 2000). Since this process is not required in this interferometer approach, the systematic error can be well below 2 m/s. Hence, Doppler precision of sub m/s is potentially reachable through increasing photons collected by each fringe and increasing wavelength coverage. We have achieved ~ 8 m/s Doppler precision with star light at the HET with an approximately ~ 140 Å wavelength coverage, a $R = 6700$ post-disperser and a S/N ~ 100 per pixel. This error is consistent with photon-noise limit².

Another exciting possibility with this interferometer technique is to extend RV surveys for planets in wavelengths other than the visible, previously not covered by echelle surveys. Since the interferometer response is simple and stable, there is no need for calibrating instrument response as for the echelle. Instrument wavelength calibrations (or instrument zero velocity drift measurements) can be conducted with reference sources with a lower line density than the iodine used in the echelle. Therefore, this instrument can be easily adapted to other wavelengths for maximizing the photon flux, and number of stellar absorption lines for precision Doppler RV measurements. The candidate stars for this potential survey include late M, L, and T dwarfs, early type B, A stars and white dwarfs. Late M, L and T dwarfs have peak fluxes in the near-IR. For instance, the late M dwarfs have peak flux in the near-IR, at least a factor 10 higher than at the visible (Kirkpatrick et al. 1993; 1999) and since a number of molecular absorption lines are concentrated in this wavelength region, observing

¹For instance, a Michelson type interferometer with corner cube mirrors can feed both interferometer outputs to the detector at $\sim 90\%$ efficiency (Traub 2002). A low resolution spectrograph using a volume phase grating can potentially reach $\sim 70\%$ transmission (Barden et al. 2000). Together with the telescope transmission ($\sim 80\%$), fiber-feed transmission ($\sim 70\%$) and detector quantum efficiency ($\sim 90\%$), the total detection efficiency can reach $\sim 30\%$. Details about the total transmission budget will be discussed in a follow-up paper (Ge et al, 2002)

²The reason that we were not able to reach higher precision is that the calibration error from using iodine reference is ~ 7 m/s, dominating the total measurement error. At $R \sim 6700$, mean fringe visibility for iodine absorption lines are too low ($\sim 2.5\%$) compared to that for stellar absorption lines ($\sim 7\%$). In the future, a calibration source with much higher fringe visibility will replace the iodine for achieving sub m/s. Details on new calibration techniques will be reported in the follow-up paper (Ge et al. 2002)

time can be significantly reduced if the IR spectra can be used for RV measurements. A and B main sequence stars have very broad intrinsic absorption lines dominated by the Balmer series due to rapid rotation. White dwarfs have very broad intrinsic absorption lines due to pressure broadening. Typical rotation velocity for normal A and B type stars is about 150 km/s, ~ 30 times faster than a typical late type star (Gray 1992; Dravins 1987). Due to the broader intrinsic line profile, the intrinsic Doppler error for these stars increases by ~ 6 times compared to the late type stars. However, with deep Balmer absorption lines over large wavelength coverage of most of the Balmer lines and high signal-to-noise ratio data, it is possible to achieve \sim a few m/s Doppler precision for detecting planets around these stars for the first time.

The author is grateful to David Erskine, Julian van Eyken, Suvrath Mahadevan, Larry Ramsey, Don Schneider, Steinn Sigurdsson, Web Traub, Ron Reynolds, Fred Roesler, Stuart Shaklan, Harvey Moseley, Bruce Woodgate, Roger Angel, Mike Shao, Chas Beichman, Ed Jenkins & Jim Gunn for stimulating discussions on this new instrument concept.

REFERENCES

- Barden, S.C, Arns, J.A., Colburn, W.S. & Williams, J.B. 2000, PASP. 112, 809
- Butler, R.P., Marcy, G.W., Williams, E., McCarthy, C., Dosanji, P., & Vogt, S. S. 1996, PASP, 108, 500
- Connes P. 1985, ApSS, 110, 211
- D’Odorico, S. et al. 2000, Proc. SPIE, 4005, 121
- Douglas, N.G. 1997, PASP, 109, 151 4
- Dravins, D. 1987, A&A, 172, 200
- Erskine & Ge 2000, in Imaging the Universe in Three Dimensions: Astrophysics with Advanced Multi-Wavelength Imaging Devices, (APS series) Edited by W. van Breugel & J. Bland-Hawthorn, 195, 510 10
- Frandsen, F., Douglas, N.G., & Butcher, H.R. 1993, A&A, 279, 310
- Gray, D.F. 1992, The Observation and analysis of stellar photospheres (Cambridge Astrophysics Series)
- Ge, J., et al. 2001, BAAS, 199, 3304 11
- Ge, J., van Eyken, J., & Mahadevan, S. 2002, to be submitted to ApJ Letters
- Goodman, J.W. 1984, Statistical Optics (A Wiley-Interscience Publication)

- Harvey, J. et al. 1995, in Gong'94: Helio- and Astro-Seismology, (APS series), Edited by R.K. Ulrich, E.J. Rhodes, Jr. & W. Dppen, 76, 432
- Kirkpatrick, D.J., et al. 1993, ApJ, 402, 643 18
- Kirkpatrick, D.J., et al. 1999, ApJ, 519, 802 19
- Kozhevato, I.E., Kulikova, E.Kh. & Cheragin, N.P. 1995, Astronomy Letters, 21, 418
- Kozhevato, I.E., Kulikova, E.H., & Cheragin, N.P. 1996, Solar Physics, 168, 251
- Suntzeff, N.B. 1994, PASP, 107, 990 15.
- Title, A.M., & Ramsey, H.E. 1980, Applied Optics, 19, 2046
- Traub, W. 2002 private communications
- Valenti, J. 2000 private communications
- Van Eyken, J., et al. 2001, BAAS, 199, 0303 12
- Vogt, S.S. et al. 1994, Proc. SPIE, 2198, 362

Figure Captions

Figure 1. – Principle of a fixed-delay interferometer and a post-disperser. The fringe data was taken with a prototype instrument, called Exoplanet Tracker (ET) and a 1kx1k CCD array, developed at Penn State (Ge et al. 2001; van Eyken et al. 2001). The stellar interference fringes, formed by a Michelson type interferometer with ~ 7 mm optical delay, lie in the horizontal direction and are sampled by ~ 60 pixels. The fringes over different wavelengths are separated by a first order diffraction grating with a resolving power of $R \sim 6,000$, a factor of ten times lower than typical echelle spectrographs and recorded in the vertical direction of the CCD.

Figure 2. – Product of delay and fringe visibility vs. delay in the interferometer for a gaussian shaped profile. The maximum for $d\gamma = 0.23D_i l_c$ is at $d = 0.37l_c$. The optimal value for delay depends on shape of the stellar line profile.

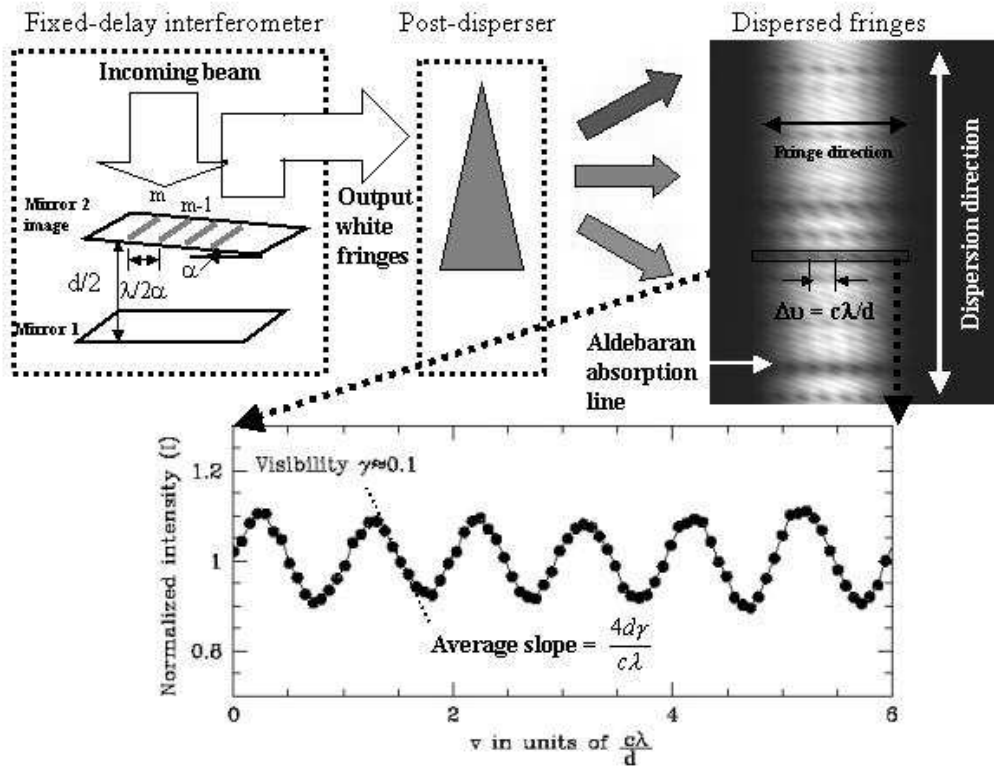


Fig. 1.—

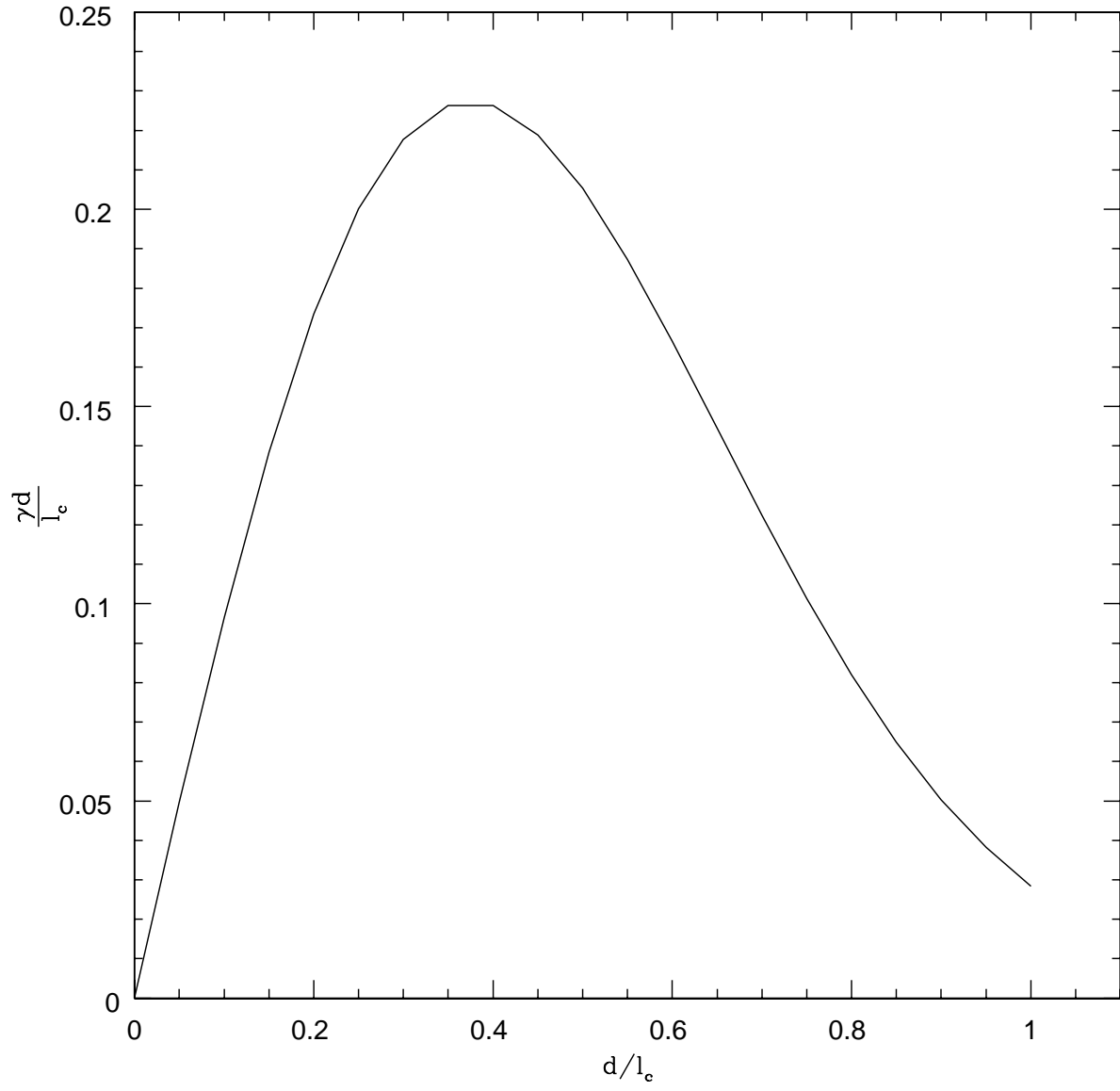


Fig. 2.—